

Effect of Slag Composition on Wettability of Oxide Inclusions

Brian Joseph MONAGHAN,¹⁾ Hamed ABDEYAZDAN,^{1)*} Neslihan DOGAN,²⁾ Muhammad Akbar RHAMDHANI,³⁾ Raymond James LONGBOTTOM¹⁾ and Michael Wallace CHAPMAN⁴⁾

1) PYROmetallurgical Research Group, School of Mechanical, Materials and Mechatronic, University of Wollongong, Wollongong, NSW 2522 Australia. 2) Department of Materials Science and Engineering, McMaster University, Hamilton, ON, L8S 4L7 Canada. 3) Faculty of Science, Engineering and Technology, Swinburne University of Technology, Hawthorn, VIC 3122 Australia. 4) BlueScope Ltd, Port Kembla, NSW 2505 Australia.

(Received on March 23, 2015; accepted on May 18, 2015; J-STAGE Advance published date: August 28, 2015)

Inclusion removal is key in the production of high quality steel. The inclusions are primarily removed from liquid steel by reacting with a liquid slag phase. For efficient inclusion removal, the inclusions transfer across the steel-slag interface to dissolve in the slag. This transfer process is strongly influenced by interfacial phenomena. In this study, the dynamic wetting (θ) of a range of slags in the CaO–Al₂O₃–SiO₂–(MgO) system on solid oxides representing inclusion phases (Al₂O₃, MgAl₂O₄ and CaO·Al₂O₃) at 1 773 K was investigated using a sessile drop technique. It was found that for all systems studied θ versus time showed a rapid decrease in wetting in the first 10 s tending to a plateau value at extended times. Further, for basic type ladle slags the plateau value was independent of slag composition and for acid type tundish slags the plateau value decreased with increasing basicity. Through work of adhesion analysis it was shown that ladle type slags appeared more suitable for inclusion removal and that from a wetting perspective calcium aluminate would be easier to remove than spinel and alumina. Choi and Lee's dynamic wetting model was evaluated and found to not only represent the data well but have physical relevance for the basic, but not the acid, slags investigated.

KEY WORDS: inclusion removal; wettability; clean steel; steel refining.

1. Introduction

Inclusion removal is key in the production of high quality steel.^{1,2)} Non-metallic inclusions in steel are formed through steel deoxidation, refractory erosion and/or corrosion as well as slag and mould flux entrainment and solidification products. These affect both productivity and the physical properties of the final product and, where they can be removed, are normally removed by reacting with a liquid oxide phase (slag). Removal is primarily achieved by optimising the process conditions to promote contact and reaction between the inclusion and slag and ultimately transfer of the inclusion from the steel to slag.²⁾

Transfer of inclusions across the steel-slag interface is strongly influenced by interfacial properties and is probably the least understood step in inclusion removal.^{2,3)} For an inclusion to be removed it must pass through the metal-slag interface and into the slag phase. This is favoured when contact angle (θ) for the steel-inclusion is greater than 90° (non-wetting) and that this value is greater than θ for the inclusion-slag ($\theta_{\text{steel-inclusion}} > \theta_{\text{slag-inclusion}}$).³⁾ In the previous work by the current authors on dynamic wetting of ladle type slags on solid MgAl₂O₄ spinel⁴⁾ it was found that increasing the basicity of the slag lowered the initial θ but had little effect on the final θ *i.e.* at extended times θ tended

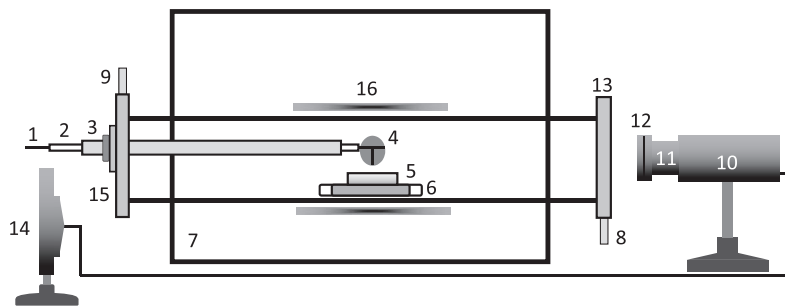
to the same value for the slags tested. Further, it was also found that the Choi and Lee spreading model⁵⁾ appeared to represent the data well and showed promise as a tool for understanding the effects of slag thermo-physical properties on wetting. It was not possible to be more definitive with respect to the model as only a limited number of slags on one substrate (spinel) was assessed.

In this study the effect of a broader range of slag compositions in the CaO–Al₂O₃–SiO₂–(MgO) system with a wider range of expected thermophysical properties on 3 substrates (alumina: Al₂O₃, spinel: MgAl₂O₄ and calcium aluminate: CaO·Al₂O₃) on the dynamic wetting behaviour was investigated.

2. Experimental

A schematic of the sessile drop apparatus used to measure the contact angle between liquid slag and a solid substrate is given in **Fig. 1**. The substrate phase was chosen to represent steel inclusion phases Al₂O₃, MgAl₂O₄ and CaO·Al₂O₃. The slag and substrate were heated separately to 1 773 K, the experimental temperature, under high purity (99.99%) argon at a flow rate of 0.75 l/min. The gas was scrubbed by passing through ascarite and drierite prior to entering the furnace. Once the temperature was stabilized (~10 minutes) the liquid slag was added to the substrate. The details of this technique have been reported elsewhere.⁴⁾ The spreading of the slag on the substrate was recorded using a Sony

* Corresponding author: E-mail: ha984@uowmail.edu.au
DOI: <http://dx.doi.org/10.2355/isijinternational.ISIJINT-2015-168>



1: Pt. wire	5: Inclusion substrate	9: Outlet gas	13: Quartz window
2: Twin bore tube	6: Tray and block	10: Camera	14: Monitor
3: Alumina support	7: Resistance furnace	11: 2x telephoto lens	15: Flange
4: Liquid slag held with Pt. wire	8: Inlet gas	12: Filters	16: Furnace hot zone

Fig. 1. A schematic of the sessile drop apparatus.

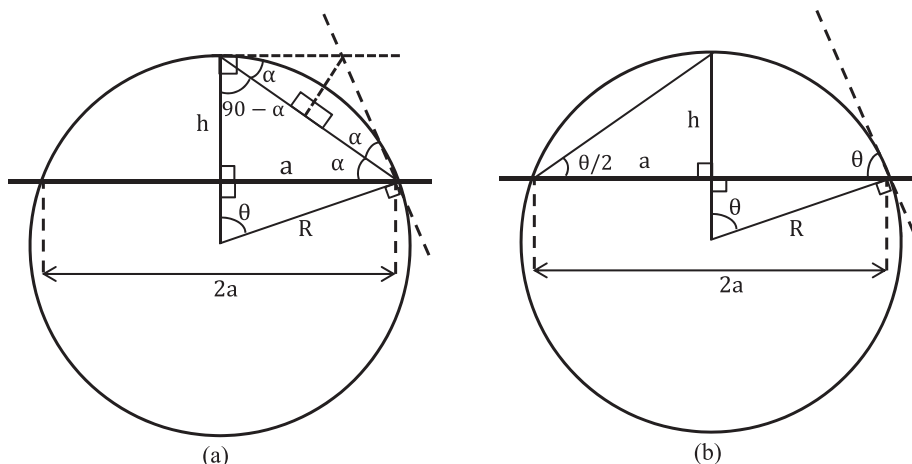


Fig. 2. (a) and (b) Showing a schematic of a sessile drop’s geometry. The drop is approximated to a spherical cap as defined by the radius of the base and height above basal plane.

6.1 MP video camera (HDR-SR7E). The camera was fitted with a 2 x telephoto lens and 2 HOYA neutral density filters (NDX4 and NDX400) in series.

The contact angle (θ) was calculated using Eq. (1) representing the geometry of a spherical cap (as can be seen in Fig. 2⁶⁾) using digital still images captured from the recordings,

$$\frac{\theta}{2} = \tan^{-1} \frac{h}{a} \dots\dots\dots (1)$$

where, R is the radius of the sphere dissected by the basal plane, h is the height of contact circle and a is radius of contact circle. The angle α in Fig. 2(a) is equivalent to $\theta/2$ in Fig. 2(b).

The slags used were prepared by mixing laboratory grade oxides CaO (CaCO₃), Al₂O₃, SiO₂ and MgO (where applicable) of appropriate proportions. These mixtures were then melted in a platinum crucible, quenched and crushed. This process was repeated twice to ensure slag homogeneity. The composition of the resultant slags, as measured by XRF, are

Table 1. Chemical composition of the experimented slags in mass%.

	Slag composition in mass%				B
	CaO	Al ₂ O ₃	SiO ₂	MgO	
T1	25.5	17.4	57.1	–	0.34
T2	32.7	19.2	48.1	–	0.49
T3	40.3	19.0	40.7	–	0.68
L1	41.8	42.7	9.2	6.3	0.81
L2	46.3	37.1	9.8	6.8	0.99
L3	50.9	32.9	9.5	6.7	1.20

given in Table 1. In Table 1, the slags T1–T3 are of compositions similar to that used in a tundish (referred to as T type in the text) and the slags L1–L3 represent ladle type slags (referred to as L type in the text). The slag basicity (B), was defined as $\frac{\text{CaO}}{\text{SiO}_2 + \text{Al}_2\text{O}_3}$ in mass ratio, is also given in the

table. From these slags, $\sim 0.2 \times 10^{-3}$ kg sintered pellets were prepared and used in the sessile drop experiments.

The Al_2O_3 substrates were supplied by Rojan Advanced ceramics, Western Australia. They were cut to a size of 30×10^{-3} m diameter for sessile drop experiments. The $MgAl_2O_4$ and $CaO \cdot Al_2O_3$ powders were prepared from high purity laboratory grade MgO , Al_2O_3 and $CaCO_3$ ($> 99\%$) starting materials by reaction sintering. The appropriate proportion of required powders were mixed and then pressed into disks and sintered at 1 873 K for spinel and at 1 723 K for calcium aluminate in a period of 24 hours. This sintered material was then crushed to a fine powder ($< 38 \mu m$) and re-sintered at 1 998 K for the former and at 1 798 K for the latter for a period of 6 hours. After the second sintering, the spinel and calcium aluminate phases were confirmed by X-ray diffraction (XRD), see **Figs. 3(a)** to **3(c)** for alumina, spinel and calcium aluminate respectively. No other phases were identified.

The alumina, spinel and calcium aluminate substrates had an average apparent porosity¹⁰⁾ of 0.5%, 1.9% and 1.7% respectively. The spinel was of composition 71.7% Al_2O_3 and 28.3% MgO and the calcium aluminate composition was 64.5% Al_2O_3 and 35.5% CaO in mass%. To minimize the effect of surface roughness all substrates were then polished to $1 \mu m$ prior to use in the sessile drop experiments.

The surface roughness of the substrates was measured by using a non-contacting surface roughness measuring apparatus (Veeco Wyko NT9100 Optical Profilometer) and the mean center-line roughness (R_a) was measured for a number of points on the substrates and an average value of $0.147 \mu m$ was obtained.

3. Results and Discussion

3.1. Wetting Behavior

A typical example of the spreading and wetting behavior of a liquid slag drop on a ceramic substrate of spinel can be found in the previous study of the current authors.⁴⁾ The liquid drop spread out on the substrate within a few seconds. This behavior was observed for all slags and substrates used. The θ decreased rapidly in the first 10 s tending to a plateau value at the extended times for slag types on different substrates. The θ reached to plateau value between ~ 30 to 70 seconds.

The initial drop in θ is consistent with the previous work the authors have reported on spinel material^{4,11)} and similar to what other workers found for $CaO-SiO_2-Al_2O_3$ based slags on alumina.⁵⁾ This change is likely to be principally due to the reaction of the slag with the substrate but may also contain a momentum component due to the slag addition technique.

The plateau θ value for L type slags was relatively independent of slag composition on all substrates. The T type slags showed a lower θ with increasing basicity of the slag, this was less pronounced for the spinel substrate. Further, it took longer for the T1 slag to reach a plateau value. This was the most acidic slag. This longer time is likely due to a combination of both the drive to equilibrium (thermodynamic factor) and resistive forces associated with the viscosity of the slag. The effect of slag viscosity is further discussed when applying the Choi and Lee⁵⁾ dynamic wet-

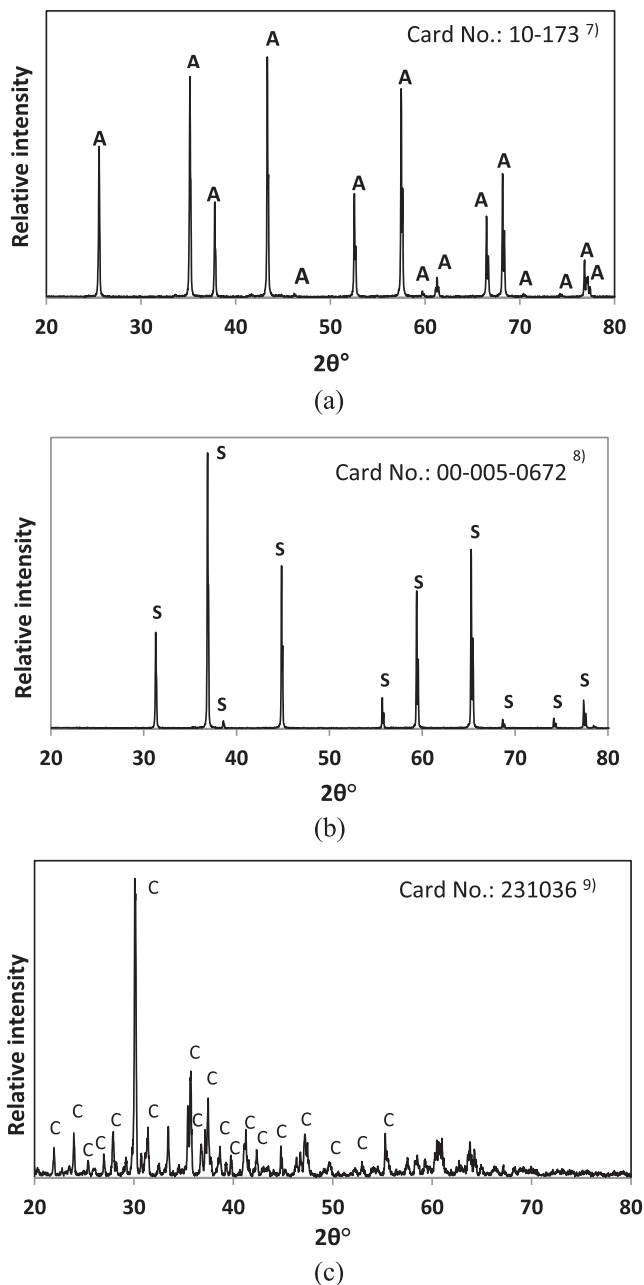


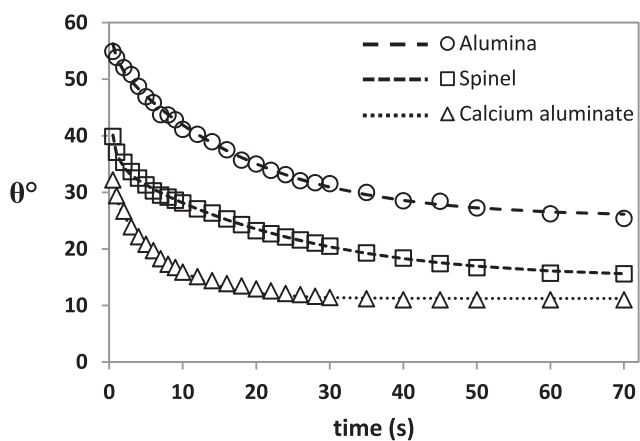
Fig. 3. The X-ray diffraction pattern for the (a) alumina (b) spinel and (c) calcium aluminate used in the preparation of the substrates. The A, S and C denote peaks as identified in the pdf cards for alumina, spinel and calcium aluminate respectively.

ting model.

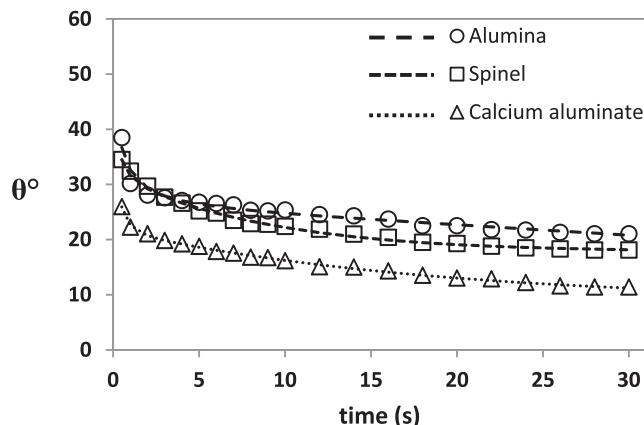
The wettability of each specific slag on different substrates was also compared and is given in **Figs. 4** and **5** for T type and L type slags respectively. It was found that θ for calcium aluminate $<$ spinel which in turn was $<$ alumina for all slags used. The concept of work of adhesion, W , has been used to assess the relative removability of different inclusion types from the steel. W was calculated via Eq. (2).⁶⁾

$$W = \sigma_{LV}(1 + \cos \theta) \dots \dots \dots (2)$$

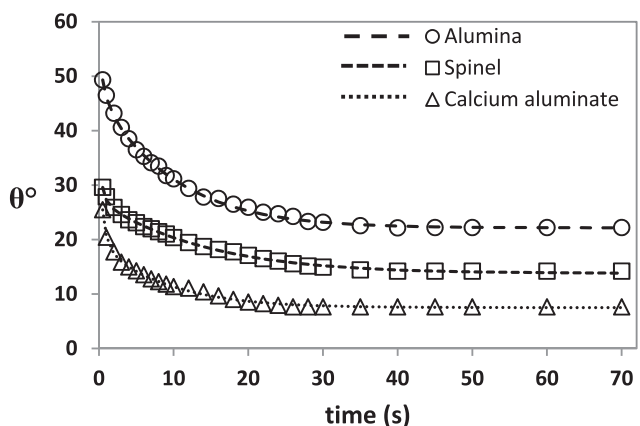
where σ_{LV} is the slag-vapor surface energy and θ is slag-substrate contact angle. The σ_{LV} values for slags used were obtained via the National Physical Laboratory (NPL) slags



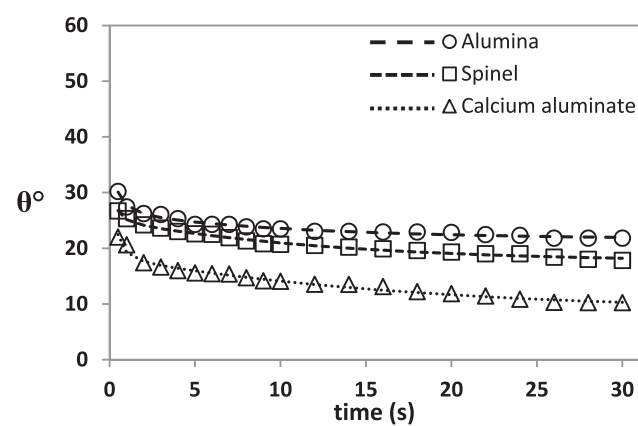
(a)



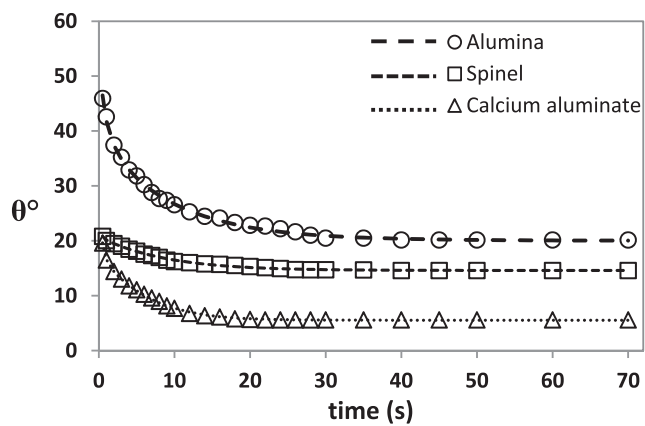
(a)



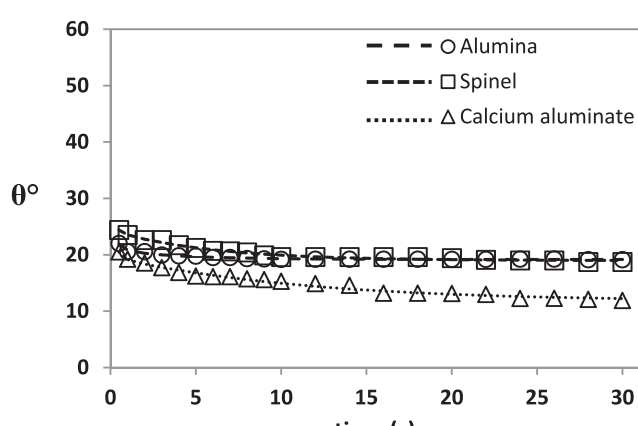
(b)



(b)



(c)



(c)

Fig. 4. Wetting behavior of (a) T1, (b) T2 and (c) T3 slag on alumina, spinel and calcium aluminate substrates. The lines represent fits of the Choi and Lee⁵⁾ model to the data.

Fig. 5. Wetting behavior of (a) L1, (b) L2 and (c) L3 slag on alumina, spinel and calcium aluminate substrates. The lines represent fits of the Choi and Lee⁵⁾ model to the data.

model¹²⁾ and plateau θ values as plotted and shown in Fig. 6 have been used to calculate W (see Fig. 7). It can be seen that the lower the θ the greater the W . From Fig. 7, it can also be seen that L type slags give a greater W than that of T type ones. The greater W is indicative of a stronger bond between slag and inclusion. This likely indicates that for all other factors being equal, the efficiency of removal of inclusions from steel is likely to be greater using L-type slags and greater for that of calcium aluminate than that of spinel and alumina.

The primary limitation in this analysis is that any inclu-

sion size/radius/morphology effects have not been addressed and that the system being studied is slag-inclusion phase-gas (Argon) as opposed to slag-inclusion phase-liquid steel. While this may limit the direct applicability to steelmaking of the experimental results and the work of adhesion approach, the data generated and analysis offers a basis for possible selection of inclusion and slag type to optimize inclusion removal.

Table 2. Fitting parameters obtained for Eq. (3).

Substrate	Slag	$\theta_{e,app}^0$	$\theta_{e,app}^\infty$	k	m
Alumina	T1	54.4	27.0	0.074	3.792
	T2	44.4	22.1	0.115	2.829
	T3	33.6	20.0	0.111	2.134
	L1	26.2	15.6	0.026	2.766
	L2	26.1	21.6	0.090	4.054
	L3	20.2	19.1	0.171	4.943
Spinel	T1	34.6	14.8	0.053	3.300
	T2	26.7	13.8	0.085	4.495
	T3	20.7	14.6	0.129	7.448
	L1	30.7	17.7	0.123	3.878
	L2	25.0	17.6	0.088	5.205
	L3	24.2	19.0	0.180	6.888
Calcium aluminate	T1	30.6	12.2	0.202	4.680
	T2	18.0	7.0	0.123	3.886
	T3	17.2	5.4	0.213	5.305
	L1	21.9	9.8	0.083	4.442
	L2	17.9	8.1	0.063	4.735
	L3	19.5	11.8	0.106	6.408

Table 3. σ_{LV} and η and calculated values of m from Eq. (4).

Slag	σ_{LV} (N/m)	η (Ns/m ²)	$m = \frac{\sigma_{LV}}{\eta}$ (m/s)
T1	0.408	7.89	0.05
T2	0.443	3.01	0.15
T3	0.472	1.09	0.43
L1	0.597	0.27	2.2
L2	0.594	0.14	4.3
L3	0.595	0.08	7.4

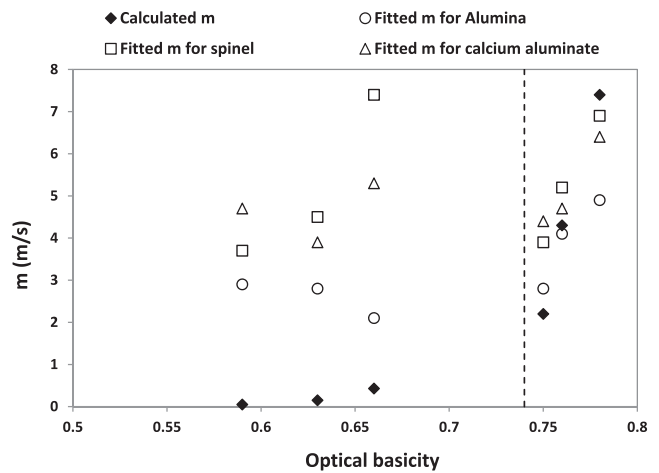


Fig. 9. The effect of slag optical basicity on calculated and fitted m for substrates used. The dashed line represents the point of neutrality for a simple CaO–SiO₂ binary slag.

from an independent method. To the authors’ knowledge these data are not available in the literature. From the Choi and Lee wetting model it is not clear exactly what k represents. It is a pre-exponential term from an Arrhenius approach to reactivity or diffusion and perhaps could be argued as a probability or jump frequency factor.¹⁵⁾ It is not at all clear how this factor would be expected to vary with changing slag composition or substrate phase and therefore how it would be used it to assess the model.

To evaluate the m parameter represented by Eq. (4) characteristic values for η and σ_{LV} of the slags were calculated using the Riboud model¹⁶⁾ and NPL slags model¹²⁾ respectively. These values are given in **Table 3** and compared with the m values obtained from the Choi and Lee model (Table 2).

There is a good agreement with the calculated and fitted m values, both in terms of order of magnitude and trend with changing slag composition, for the type L slags on all 3 substrates. With the T type slags there is no obvious relation between the different (calculated and fitted) m values. The choice of slags studied was based on those reported for use in steelmaking processes¹⁷⁾ and also to ensure that a broad range of viscosities, and hence parameter m would be evaluated. The type T slags are acid like *i.e.* they are large covalently bonded ions, whereas the type L slags have a basic character and smaller ions. To assess or infer the effect of structure of the slag on parameter m, a plot of m versus optical basicity (Λ) was evaluated and given in **Fig. 9**. Λ was calculated using Eq. (5)

$$\Lambda = X_i \Lambda_i + X_j \Lambda_j + X_k \Lambda_k + \dots \dots \dots (5)$$

where Λ_i is the optical basicity value of the single oxide and X is the equivalent cation fraction of each oxide. The

values used for Λ_i are those recommended in the review by Sommerville and Yang.¹⁸⁾ There is no universally applicable model that deals with slag structure from acid through to basic slags that is fully quantitative,¹⁹⁾ the choice of optical basicity is purely for convenience.

From Fig. 9, it can be clearly seen the two populations of data, the basic slag (values of $\Lambda > 0.75$), showing a strong correlation between calculated and fitted m and changes in m with basicity and the acid slag (values of $\Lambda < 0.660$) showing little correlation in m or m with basicity.

Why should there be such a difference in the predicted value with respect to slag structure? As stated previously the m parameter represents a simple force balance between viscosity and interfacial forces. This force balance appears to be adequate for the simple basic slags but not so for the more complex acidic slags. Acid slags potentially have large more complex ions than basic slags, they may be ring structures and or long chain ions built from the Si tetrahedron.^{20,21)} Basic slags contain ions based on the simple Si tetrahedron, basic cations and excess O²⁻ ions.^{20,21)} The large structures associated with acid slags require greater shear forces than basic slags to induce movement resulting in an increased viscosity. Further, these more complex acid slag structures are likely to present a more variable ion surface to the gas or solid interface than the relatively simple basic slag.²⁰⁾ It is likely the more complex interface and the effects of the larger acid ion structures are not fully represented in viscosity and/or are not simply resolved for the interfacial forces and that other terms may have to be

considered. While it has not been shown that Choi and Lee model has applicability in acid slags it would appear to offer much promise in basic slag systems.

4. Conclusions

In a study to investigate the dynamic wetting of selected slags in the CaO–Al₂O₃–SiO₂–(MgO) system on alumina, spinel and calcium aluminate substrates it was found that

- The θ of the slags for all systems studied showed a rapid decrease in wetting in the first 10 s tending to a plateau value at extended times. Further, that for basic type ladle slags the plateau value was independent of slag composition and for acid type tundish slags the plateau value decreased with increasing basicity.
- For the slags systems tested it was found that θ for calcium aluminate < spinel which in turn was < alumina.
- From a work of adhesion analysis it was found that for all other factors being equal ladle type slags would show better inclusion removal characteristics for the phases tested and that from a wetting perspective calcium aluminate would be easier removed than spinel and alumina.
- Choi and Lee's dynamic wetting model was evaluated and found to not only represent the data well but have physical relevance for the basic but not for the acid slags tested.

Acknowledgments

The authors acknowledge the support of BlueScope, the use of the Australian Research Council funded JEOL-JSM6490 LV SEM at the UOW Electron Microscopy Centre and the help of Corentin Bourgeois for his assistance in this work.

REFERENCES

- 1) J. H. Lowe and A. Mitchell: Clean Steel, Institute of Materials, London, (1995), 223.
- 2) B. Deo and R. Boom: Fundamentals of Steelmaking Metallurgy, Prentice Hall International, New York, (1993), 254.
- 3) Fundamentals of Metallurgy, ed. by S. Seetharaman, Woodhead Publishing in Materials Cambridge, England, (2008), 23.
- 4) H. Abdeyazdan, N. Dogan, M. A. Rhamdhani, M. W. Chapman and B. J. Monaghan: *Metall. Trans. B*, **46B** (2015), 208.
- 5) J. Y. Choi and H. G. Lee: *ISIJ Int.*, **43** (2003), 1348.
- 6) N. Eustathopoulos, M. G. Nicholas and B. Drevet: Wettability at High Temperatures, Elsevier, New York, (1999), 106.
- 7) J. G. Swanson and R. K. Fuyat: *Circulation*, **539** (1960), No. 9, 3.
- 8) J. G. Swanson and R. K. Fuyat: *Circulation*, **539** (1953), No. 11, 35.
- 9) D. N. Baldock, P. J. Baldock, A. Parker and I. Sladdin: *J. Appl. Crystallogr.*, **3** (1970), 188.
- 10) A. 1774.5 Method 5, The Determination of Density Porosity and Water Adsorption in Refractories and Refractory Materials, Standards Australia, Canberra, (2004).
- 11) H. Abdeyazdan, N. Dogan, M. A. Rhamdhani, M. W. Chapman and B. J. Monaghan: Materials Science and Technology Conf., AIST, Warrendale, PA, (2013), 507.
- 12) K. C. Mills: Slag model, 1.07 Ed., National Physical Laboratory, UK, (1991).
- 13) L. W. Schroeder: Contact Angle, Wettability and Adhesion, VSP Utrecht, Netherland, (1993), 349.
- 14) Excel, Microsoft Office, version 14.0.6106.5005, (32-bit), Microsoft Office Corporation, Redmond, WA, US, (2010).
- 15) G. H. Geiger and D. R. Poirier: Transport Phenomena in Metallurgy, Addison-Wesley Publishing Company, Reading, Mass, (1973), 439.
- 16) V. Riboud, Y. Roux, L. Lucas and H. Gaye: *Fachberichte Hüttenpraxis Metallweiterverarbeitung*, **19** (1981), 859.
- 17) M. Valdez, K. Prapakorn, A. W. Cramb and S. Sridhar: *Ironmaking Steelmaking*, **29** (2002), 47.
- 18) I. D. Sommerville and Y. Yang: *The AusIMM Proc.*, **306** (2001), 71.
- 19) K. C. Mills: Slag Atlas, 2nd ed., Verlag Stahleisen GmbH, D-Düsseldorf, (1995), 10.
- 20) E. T. Turkdogan: Physicochemical Properties of Molten Slags and Glasses, The Metals Society, London, (1983), 69.
- 21) F. D. Richardson: Physical Chemistry of Melts in Metallurgy, Vol. 1, Academic Press Inc. Ltd., London, (1974), 78.